

D. BOCHENEK*, P. NIEMIEC*, R. ZACHARIASZ*, A. CHROBAK**, G. ZIÓŁKOWSKI**

FERROELECTRIC-FERROMAGNETIC COMPOSITES BASED ON PZT TYPE POWDER AND FERRITE POWDER

FERROELEKTRYCZNO-FERROMAGNETYCZNE KOMPOZYTY NA BAZIE PROSZKU TYPU PZT ORAZ PROSZKU FERRYTOWEGO

A ferroelectric-ferromagnetic composites based on PZT powder have been obtained in presented work. The main aim of combination of ferroelectric and magnetic powders was to obtain material showing both electric and magnetic properties. Ferroelectric ceramic powder (in amount of 90%) was based on the doped PZT type solid solution while magnetic component of the composite was nickel-zinc ferrite $\text{Ni}_{1-x}\text{Zn}_x\text{Fe}_2\text{O}_4$ (in amount of 10%). The synthesis of components of ferroelectric-ferromagnetic composite was performed using the solid phase sintering. Final densification of synthesized powder has been done using free sintering.

For obtained of ferroelectric-ferromagnetic composites the XRD, the microstructure, EDS, dielectric, magnetic, internal friction and electrical hysteresis loop investigations were performed. Obtained results shown the correlations between the magnetic subsystem and the electrical subsystem of the ferroelectric-ferromagnetic composites. Such properties of obtained composites give the possibility to use them in memory applications of new type.

Keywords: ferroelectromagnetics, ferroelectric-ferromagnetic composites, PZT type materials, ferrites

W pracy otrzymano ferroelektryczno-ferromagnetyczne kompozyty na bazie ceramicznego proszku typu PZT. Połączenie ferroelektrycznego i magnetycznego proszku miało na celu otrzymanie materiałów wykazujących zarówno elektryczne i magnetyczne właściwości. Ferroelektryczny, ceramiczny proszek (w ilości 90%) stanowiły domieszkowane składki proszku typu PZT, natomiast magnetycznym składnikiem w kompozycie był niklowo-cynkowy ferryt ($\text{Ni}_{1-x}\text{Zn}_x\text{Fe}_2\text{O}_4$). Syntetyzowanie składników kompozytu ceramiczno-ferrytowego przeprowadzono metodą spiekania wyprasek w fazie stałej, natomiast zagęszczanie zsintetyzowanego kompozytowego proszku metodą spiekania swobodnego.

Przeprowadzono badania rentgenowskie, mikrostrukturalne, EDS, dielektryczne, magnetyczne, tarcia wewnętrznej oraz elektrycznej pętli histerezy. Badania wykazały, występowanie korelacji między podukładem magnetycznym i podukładem elektrycznym w ferroelektryczno-ferromagnetycznych kompozytach. Dzięki ferroelektrycznym i magnetycznym właściwościom otrzymanych kompozytów, materiały tego typu mogą znaleźć zastosowanie aplikacyjne w nowych typach pamięci.

1. Introduction

$\text{PbZr}_{1-x}\text{Ti}_x\text{O}_3$ ceramics (PZT) belongs to a family of multicomponent solid solutions type $(1-x)\text{PbZrO}_3-(x)\text{PbTiO}_3$ that present broad isomorphism which allows for doping the base composition in position A and B by various foreign component with various foreign ions [1-3]. At room temperature, the solid solution of PZT have two ferroelectric phases, a tetragonal phase on the titanium rich side of the pseudobinary system and a rhombohedral one on the zirconium rich side. The best of dielectric and piezoelectric properties can be found in ceramics with compositions near $\text{Pb}(\text{Zr}_{0.53}\text{Ti}_{0.47})\text{O}_3$, which corresponds to the tetragonal-rhombohedral phase transition [4].

Optimization of a technological process (technological conditions), a selection of the PbTiO_3 concentrations (in the solid solution of a PZT type) and also a modification of the basic chemical composition with appropriate admixtures al-

lows for producing ceramics for numerous applications in various types of piezoelectric transducers, electric band filters, as sensors, generators, servomotors, phase modulators, frequency multipliers, filters, electromechanical, electroacoustic, pyroelectric transducers, memory elements, etc [5-8].

The nickel-zinc ferrite ($\text{Ni}_{0.64}\text{Zn}_{0.36}\text{Fe}_2\text{O}_4$), belonging to so-called soft ferrites with high magnetic permeability and high resistance (working frequency within the range of 50–1,000 MHz) [9], is used during signal processing (telecom filters, proximity sensors, delay lines), in EMI filters and wide-band transformers, among others.

The aim of the work was to obtain ferroelectric-ferromagnetic composites based on a PZT type ferroelectric powder and nickel-zinc ferrite, as well as to test their basic properties, including the correlation between magnetic and electric subsystems in composites.

* UNIVERSITY OF SILESIA, DEPARTMENT OF MATERIALS SCIENCE, ŚNIEŻNA 2, 41-200 SOSNOWIEC, POLAND

** UNIVERSITY OF SILESIA, INSTITUTE OF PHYSICS, UNIWERSYTECKA 14, 40-007 KATOWICE, POLAND

2. Experiment

For the purpose of obtaining ferroelectric-ferromagnetic composites, PZT type powder was used with ferroelectric properties as well as nickel-zinc ferrite powder ($\text{Ni}_{0.64}\text{Zn}_{0.36}\text{Fe}_2\text{O}_4$) with ferromagnetic properties. The ferroelectric components were two PZT type compositions: $\text{Pb}_{0.90}\text{Ba}_{0.10}(\text{Zr}_{0.53}\text{Ti}_{0.47})\text{O}_3 + 2\% \text{at. Nb}_2\text{O}_5$ (PBZTN) and $\text{Pb}_{0.94}\text{Sr}_{0.06}(\text{Zr}_{0.46}\text{Ti}_{0.54})\text{O}_3 + 0.25\% \text{at. Cr}_2\text{O}_3$ (PSZTC). The initial constituents for obtaining PZT type powders were oxides: PbO , ZrO_2 , TiO_2 , Nb_2O_5 , Cr_2O_3 as well as carbonates: barium BaCO_3 and strontium SrCO_3 . The main component of the composite – ceramic PZT type powder – was synthesized using sintering of a mixture of simple oxides in solid phase (compaction by free sintering) under the following conditions: $T_{\text{synth}} = 850^\circ\text{C}$, $t_{\text{synth}} = 2$ h.

The second element of the composite having ferromagnetic properties (ferrite powder $\text{Ni}_{0.64}\text{Zn}_{0.36}\text{Fe}_2\text{O}_4$) was synthesized using calcination under conditions of $1100^\circ\text{C}/4$ h.

The synthesized ceramic powder constituted 90%, while the ferrite powder – 10%, of the PZT-NiZn composite. After proportionally weighing and mixing components, synthesizing was carried out using sintering of the mixture of simple oxides in a solid phase (compaction by a free sintering method) under the following conditions: $T_{\text{synth}} = 1050^\circ\text{C}$ and $t_{\text{synth}} = 4$ h. Final densification of the synthesized composite powder was carried out using free sintering method under the following conditions: $T_s = 1250^\circ\text{C}/t_s = 2$ h. Two ferroelectric-ferromagnetic composites were obtained, marked in the following way: PBZTN-NiZn, PSZTC-NiZn. Silver electrodes were applied to surfaces of composite samples for the purpose of carrying out electric tests.

The X-ray studies of the crystallographic structure were performed by means of a Philips X'Pert diffractometer. Microstructure tests were carried out using a scanning electron microscope HITACHI S-4700 with a field emission with EDS Noran Vantage system. Magnetic properties measurements were performed on the magnetometer SQUID (MPMS XL-7 Quantum Design) in the range of temperatures from -271°C to 27°C (used magnetic field to 7 T) and a magnetic Faraday balance in the range of temperatures from 27°C to 827°C .

Temperature measurements of dielectric parameters were made using a QuadTech 1920 Precision LCR Meter. Hysteresis (P - E) loops at various electric field frequencies were investigated with a Sawyer-Tower circuit and a Matsusada Inc. HEOPS-5B6 precision high voltage amplifier. Data were stored on a computer disc using an A/D, D/A transducer card. The measurements of the temperature dependences of internal friction $Q^{-1}(T)$ and temperature dependences of Young's Modulus $Y(T)$ were performed by automatic resonance mechanical spectrometer of the RAK-3 type controlled by computer.

3. Results and discussion

Fig. 1a presents X-ray spectra of synthesized PZT type (PBZTN and PSZTC) powders at room temperature. The PZT type phases could be identified from X-ray peaks in a range of 2θ from 42° to 47° , which corresponded to a $(020)_R$ reflex-

tion of rhombohedral (R) structure and double $(200)_T$ – $(002)_T$ peaks of tetragonal (T) structures. The X-ray investigations of the PSZTC ceramics (Fig. 1a) confirmed that the material have a perovskite type structure from morphotropic area (near the tetragonal phase). The PBZTN ceramics have a perovskite type structure from morphotropic area (near the rhombohedral phase). The coexistence of phases is proven by reflexes from the rhombohedral (JCPDS no. 73-2022) and tetragonal phase (JCPDS no. 33-0784). In the case of the PBZTN graph, the presence of a triplet $(002)/(200)/(020)$ is highly dispersed. The X-ray diffraction patterns for the ferrite powder NiZnFe shows a typical single phase cubic spinel structure.

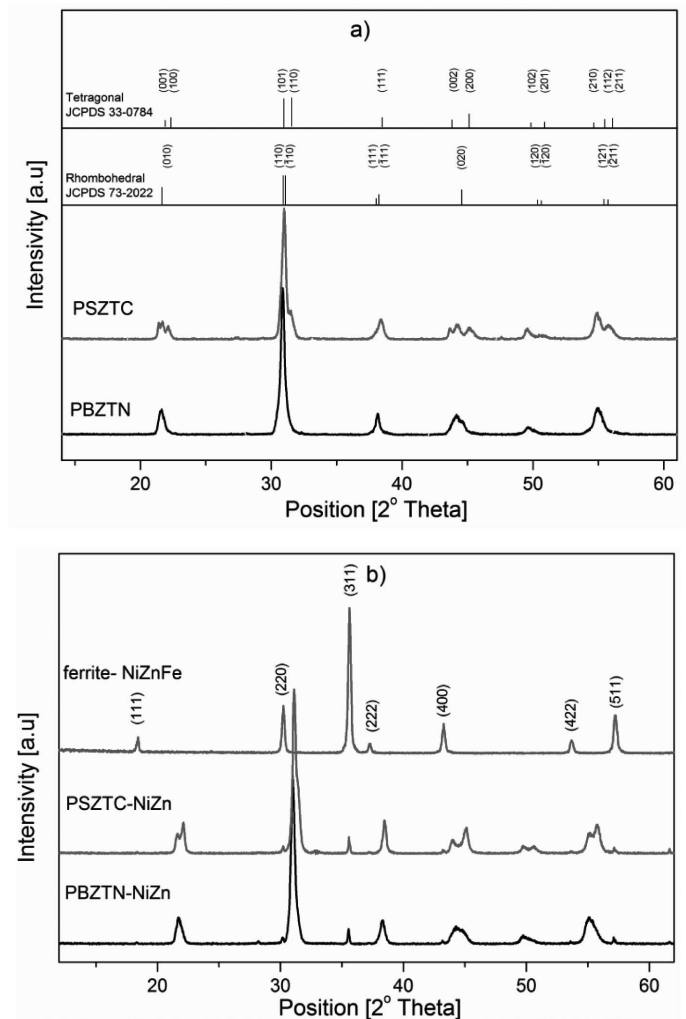


Fig. 1. 1 X-ray spectra of the PZT type powders (a) and PZT-NiZn composites (b)

An X-ray analysis of ferroelectric-ferromagnetic composite samples confirmed the occurrence of strong maxima from specific PZT type material phases as well as weak reflexes from the ferrite component (Fig. 1b). In the case of PSZTC-NiZn composite, maxima from the tetragonal phase become more clear compared to “pure” PSZTC ceramics. An X-ray analysis of PZT-NiZn composites confirmed also the lack of foreign phases.

An EDS analysis of the tested composite samples confirmed the assumed percentage share of specific components and the occurrence of elements of the ferrite and ferroelectric PZT type powders in the composite constitution (Fig. 2).

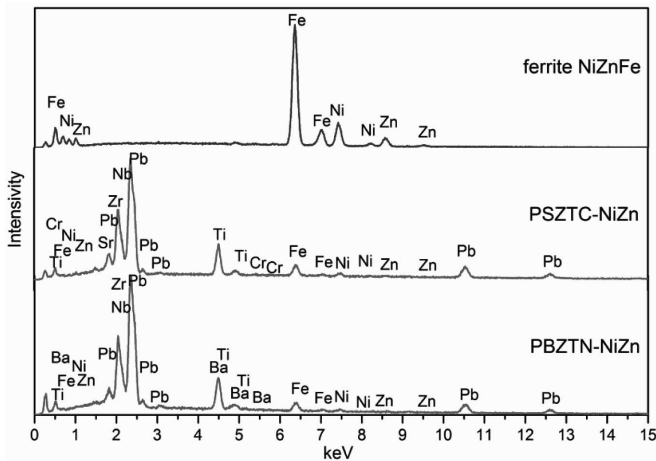


Fig. 2. EDS analysis of element breakdown for PBZTN-NiZn, PSZTC-NiZn and ferrite NiZnFe

Fig. 3 presents microstructural SEM images of PZT-NiZn type composite sample fractures. In the PBZTN-NiZn composite, there are larger grains of the ferroelectric powder show irregular grain boundaries and smaller grains of the magnetic ferrite with more regular crystals (Fig. 3a). A mixed nature of fractures occurs in this material, i.e. along boundaries as well as through grains (the occurrence of intergranular or interphase boundaries in the material).

In the case of the PSZTC-NiZn composite, the microstructure shows clear grain boundaries. Smaller ferrite grains are surrounded by larger grains of the ferroelectric component (Fig. 3b). The fracture along the grain boundaries is becoming dominating in this composite which indicates that any pollutants in the form of excessive admixtures are located at intergranular boundaries. Cations of the admixture of chromium Cr inhibit the grain growth of the ceramics during the sintering process as a result of their weak solubility in the crystalline lattice of the solid solution. The part of the admixture's cations which is not dissolved in the crystalline lattice is accumulated at grain boundaries, maintaining growth. The presence of a precipitate at grain boundaries leads to the increase in binding of neighboring grains and to the value growth of elastic constants and mechanical resistance [10].

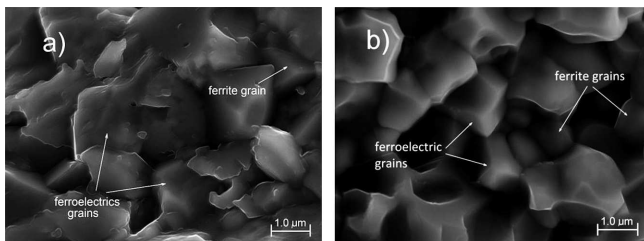


Fig. 3. SEM images of the fracture microstructure of PZT-NiZn composite samples: a) PBZTN-NiZn, b) PSZTC-NiZn

The spatial distribution of microstructure phases depends on the technology, kinetics of phase transitions, conditions of grain growth, sintering time, etc. The boundary layer between grains is not unequivocally glassy but differs from crystallites creating grains in the concentration of noise, energy, chemical and phase composition. It may comprise very small defected crystallites in which the solubility of pollutants is different than in the neighboring large crystallites. Due to all these

factors, the boundary layer differs from the inside of the grain in electric conduction and permittivity, among other things.

Tests of dielectric properties of ferroelectric-ferromagnetic composites showed the occurrence of maxima from the phase transition (Fig. 4). Temperature changes of electric permittivity ϵ ($f = 1$ kHz) for PBZTN and PSZTC ceramics are typical for multicomponent ceramics from the PZT family of materials (Fig. 4 – dashed line). The magnetic component in PZT-NiZn type composites leads to the decrease of the maximum value of electric permittivity and to a considerable diffusion of the phase transition. The diffusion of the phase transition of the electric subsystem may be an indication of the impact of magnetic properties on the electric subsystem.

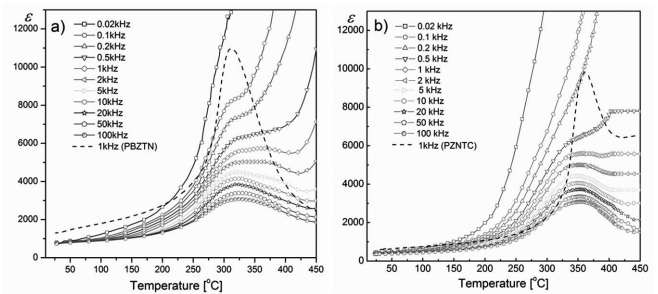


Fig. 4. Temperature relations of electric permittivity ϵ for the composite: a) PBZTN-NiZn, b) PSZTC-NiZn (heating)

In both composites, the magnetic component also leads to the increase of dielectric losses (Fig. 5) when compared to the PZT type ceramics (dashed line). Together with the increase of the measuring field's frequency, dielectric losses in composites are decreased. The PBZTN-NiZn composite has lower dielectric losses compared to the PSZTC-NiZn composite.

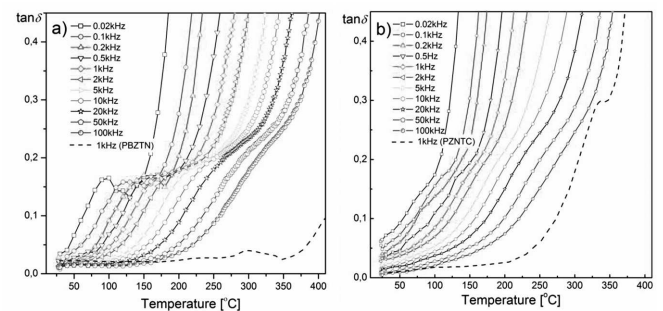


Fig. 5. Temperature relations of the $\tan \delta$ for composite: a) PBZTN-NiZn, b) PSZTC-NiZn (heating)

Temperature magnetization dependences $M(T)$, in the external magnetic field 0.1 T, of ferroelectric-ferromagnetic composites have similar courses (Fig. 6a,b); however, the PBZTN-NiZn composite has higher values of saturation magnetization M_s compared to the PSZTC-NiZn composite (Table 1). Magnetic hysteresis loops $M(H)$ of obtained PZT-ferrite composites are characteristic for soft ferromagnetic materials (Fig. 6a,b – insert graph on the right). $M(T)$ curves contain two components, i.e. a ferro/ferromagnetic one with a Curie temperature close to 400°C, and a para/superparamagnetic one which is clearly visible at temperatures below -173°C. This shows that the composite sample volumes contain not only large grains with domains of a ferromagnetic ordering, but

also smaller (non-impacting) grains which show para or superparamagnetic properties.

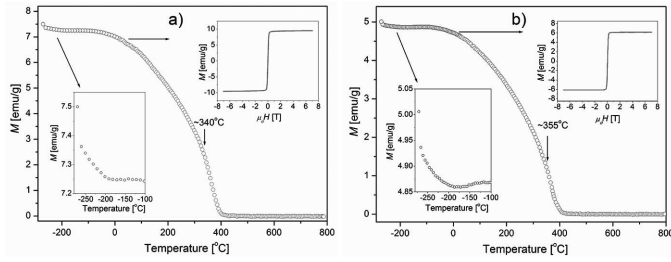


Fig. 6. Magnetization temperature dependencies for composites: a) PBZTN-NiZn, b) PSZTC-NiZn. Inset graph on the right – magnetic hysteresis loops at 27°C

TABLE 1

Parameters ferroelectric-ferromagnetic composites PZT-NiZn type (dielectric parameters for $f = 1$ kHz)

	PBZTN-NiZn	PSZTC-NiZn
ρ [g/cm ³]	7.31	7.22
$\rho_{DC} \times 10^{-6}$ at T_r [Ωm]	1.56	1.53
T_m [°C]	340	355
ϵ_r	750	350
ϵ_m	5,700	5,600
$\tan\delta$ at T_r	0.014	0.031
$\tan\delta$ at T_m	1.87	13.8
P_R [μC/cm ²]	1.74	1.47
E_C [kV/mm]	1.01	1.01
M_S [emu/g]	9.31	6.15

At a temperature of approx. 340°C (for PBZTN-NiZn) and approx. 355°C (for PSZTC-NiZn) in the area of ferroelectric-paraelectric phase transitions, changes of slope curves on the graphs $M(T)$ are observed. This behavior may be an indication of the impact of the electric subsystem on the magnetic properties of ferroelectric-ferromagnetic composites. At a temperature above 400°C, PZT-NiZn type composites are paramagnetics.

The phase transitions occurring in the PZT-NiZn type composites are visible also on the temperature dependences of the mechanical losses $Q^{-1}(T)$, determined by the internal friction method (Fig. 7). For both composites, on the dependences $Q^{-1}(T)$ in the temperature range from 250°C to 410°C, clear increase of the mechanical losses values with strong diffusing region is observed. Simultaneously, on the temperature dependences of the Young's modulus $Y(T)$, the characteristic minimum (in the temperature about 340°C for the PBZTN-NiZn composite and about 355°C for the PSZTC-NiZn composite) and next its growth is observed. Such behavior confirms occurrence in this temperature area the phase transitions. Considerable diffuseness of the mechanical losses on the dependences $Q^{-1}(T)$ is connected with overlapping two phase transitions, occurring in the PZT-NiZn composites: the phase transition of the electric subsystem and magnetic subsystem. The results

of the dielectric and magnetic investigations presented on the Figures 4 and 6, confirmed its.

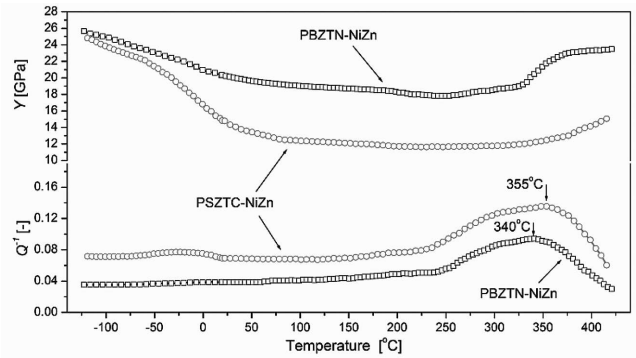


Fig. 7. Diagrams of the $Q^{-1}(T)$ and $Y(T)$ relationship for composites: a) PBZTN-NiZn, b) PSZTC-NiZn

For both composites, below 250°C, on the $Q^{-1}(T)$ as well as $Y(T)$ dependences anomalies showing about occurrence another phase transitions does not was observed. The PBZTN-NiZn composite shows lower values of the mechanical losses Q^{-1} as well as higher values of the Young's modulus Y in comparison with the PSZTC-NiZn composite. It shows that the mechanical properties are better for PBZTN-NiZn composite.

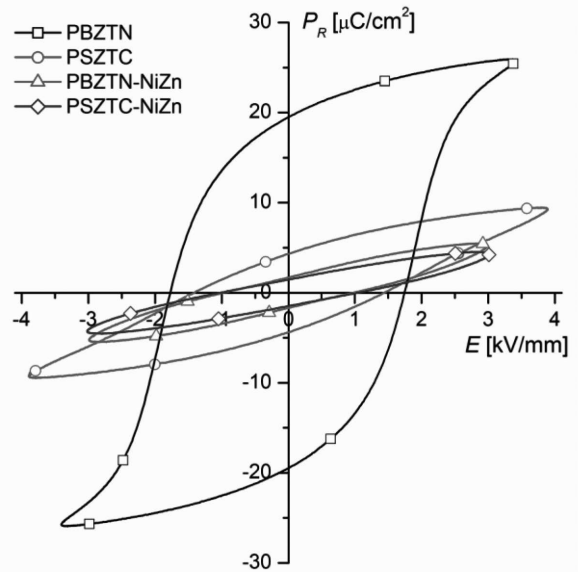


Fig. 8. Hysteresis loops for the PBZTN, PSZTC, PBZTN-NiZn and PSZTC-NiZn samples

Fig. 8 presents obtained at room temperature for ($f = 1$ Hz) electric hysteresis loops for PZT type ceramics and for ferroelectric-ferromagnetic composites. The PBZTN material belongs to the group of materials with an average ferroelectric hardness ($P_R = 19.65 \mu\text{C}/\text{cm}^2$, $E_C = 1.76$ kV/mm). A soft admixture (Nb) decreases the so-called ferroelectric hardness of the PZT piezoceramics and the consequence of such soft doping of PZT is the creation of lead vacancies in the crystalline lattice. On the other hand, PSZTC ceramics has a hysteresis loop characteristic for linear dielectrics with small losses ($P_R = 4.32 \mu\text{C}/\text{cm}^2$, $E_C = 1.42$ kV/mm). Obtained hysteresis loops of both types of PZT-NiZn composites, compared to ceramics, show similar shapes but have lower values

of residual polarization and coercion fields – TABLE 1. $P(E)$ dependences of ferroelectric-ferromagnetic composites have shape characteristic for linear dielectrics with losses.

4. Summary

An X-ray analysis of PZT-NiZn type composites confirmed the occurrence of phases from the ferroelectric and magnetic components (without the presence of foreign phases). The microstructure of ferroelectric-ferromagnetic composites comprises small grains of the ferrite element, surrounded by larger grains of the PZT type ferroelectric element.

The change of the Zr/Ti percentage share as well as the selection of suitable admixtures when creating multi-component solid solutions based on PZT allows for controlling their final usable parameters. These specific properties of the PZT type ceramic powder, combined with the magnetic ferrite powder ($\text{Ni}_{0.64}\text{Zn}_{0.36}\text{Fe}_2\text{O}_4$), allow for creating ferroelectric-ferromagnetic composites for various applications.

Complex tests of ferroelectric-ferromagnetic composite samples showed the coexistence of ferroelectric and magnetic properties. This creates possibilities for applying this type of composites in creating magnetoelectric transducers.

Acknowledgements

We are grateful for the assistance of Mgr Anna Łatkiewicz (Laboratory of FE Scanning Microscopy and Microanalysis, Institute of

Geological Sciences, Jagiellonian University, Krakow, Poland) for her help with the SEM pictures and XRD measurements.

REFERENCES

- [1] E.G. Fesenko, A.Ya. Danciger, O.N. Rozumovskaya, *Novye piezokeramicheskie materialy*, RGU, Rostov-na-Donu, 1983.
- [2] L. Kozielski, M. Adamczyk, M. Pawelczyk, *Phase Transit.* **83**, 10-11, 790-799 (2010).
- [3] R. Zachariasz, D. Bochenek, K. Dziadosz, J. Dudek, J. Ilczuk, *Arch. Metall. Mater.* **56**, 4, 1217-1222 (2011).
- [4] M.R. Soares, A.M.R. Senos, P.Q. Mantas, *J. Eur. Ceram. Soc.* **20**, 321 (2000).
- [5] D. Pandey, A.K. Singh, S. Baik, *Acta Crystall.* **A64**, 192 (2008).
- [6] E. Nogas-Cwikiel, *Arch. Metall. Mater.* **56**, 4, 1065-1069 (2011).
- [7] Y. Xu, *Ferroelectric materials and their applications*, North-Holland, Amsterdam, 1991.
- [8] W. Long, W. Ching-Chuang, W. Tien-Shon, L. His-Chuan, *J. Phys. C: Solid State Phys.* **16**, 14, 2813-2821 (1983).
- [9] M.P. Reddy, W. Madhuri, N. Ramanohar-Reddy, K.V. Siva-Kumar, V.R.K. Murthy, R. Ramakrishna-Reddy, *J. Electroceram.* **28**, 1-9 (2012).
- [10] Z. Surowiak, D. Bochenek, *Materiały ceramiczne/Ceramic Materials* **4**, 124-134 (2004).